

## Min-/Max-Volume Roofs Induced by Bisector Graphs of Polygonal Footprints of Buildings

Günther Eder\*, Martin Held<sup>†</sup> and Peter Palfrader<sup>‡</sup>

Universität Salzburg  
FB Computerwissenschaften  
5020 Salzburg, Austria  
\*geder@cosy.sbg.ac.at  
<sup>†</sup>held@cosy.sbg.ac.at  
<sup>‡</sup>palfrader@cosy.sbg.ac.at

Received 13 July 2017  
Revised 24 April 2018  
Published 12 April 2019  
Communicated by C. Knauer

Piecewise-linear terrains (“roofs”) over simple polygons were first studied by Aichholzer *et al.* (J. UCS 1995) in their work on straight skeletons of polygons. We show how to construct a roof over the polygonal footprint of a building that has minimum or maximum volume among all roofs that drain water. Our algorithm for computing such a roof extends the standard plane-sweep approach known from the theory of straight skeletons by additional events. For both types of roofs our algorithm runs in  $\mathcal{O}(n^3 \log n)$  time for a simple polygon with  $n$  vertices.

*Keywords:* Bisector graphs; roof model; straight skeleton; natural roof; realistic roof.

### 1. Introduction

In 1995, Aichholzer *et al.*<sup>1</sup> introduced straight skeletons of simple polygons. In a nutshell, the straight skeleton of a simple polygon is the geometric graph whose edges are the traces of vertices of inwards wavefronts (i.e., mitered offsets) of the polygon. The work by Aichholzer *et al.*<sup>1</sup> also highlights the intimate connection between the straight skeleton of a polygon in the two-dimensional plane and a three-dimensional structure: By embedding the wavefront propagation into three-dimensional space where the  $z$ -axis is time, the wavefront traces out a three-dimensional shape which is called the *roof*.

The study of roofs and their relation to straight skeletons is much older though, and dates back to the work by von Peschka<sup>2</sup> in the late 19th century. Aichholzer *et al.*<sup>1</sup> are the first in modern computational geometry to study bisector graphs and

This is an Open Access article published by World Scientific Publishing Company. It is distributed under the terms of the Creative Commons Attribution 4.0 (CC-BY) License. Further distribution of this work is permitted, provided the original work is properly cited.

the roof model in an attempt to work out properties of straight skeletons and to devise an algorithm for computing them. Their algorithm employs what is effectively a plane-sweep approach to compute the straight skeleton of a simple polygon with  $n$  vertices in  $\mathcal{O}(n^2 \log n)$  time and  $\mathcal{O}(n^2)$  space. Eppstein and Erickson<sup>3</sup> improve this sweep algorithm using a faster way to determine the event points. Their approach computes the straight skeleton in  $\mathcal{O}(n^{1+\varepsilon} + n^{8/11+\varepsilon} \cdot r^{9/11+\varepsilon})$  time and space for a polygon with a total of  $n$  vertices out of which  $r$  vertices are reflex, for any fixed  $\varepsilon > 0$ . Recently, Cheng *et al.*<sup>4</sup> reduced the complexity for straight skeletons over non-degenerate polygons to  $\mathcal{O}(n(\log n) \log r + r^{4/3+\varepsilon})$  time, with  $\varepsilon > 0$ .

Since every straight skeleton of a simple polygon has a corresponding roof,<sup>1</sup> it seems natural to study also other types of roofs. Indeed, so-called *realistic roofs* were introduced in recent work by several authors.<sup>5,6</sup> Their approach enumerates all possible realistic roofs over a rectilinear polygon in  $\mathcal{O}(n^5)$  time. A side result of their work is the computation of a realistic roof that has minimum height or minimum volume.

We pick up this lead and generalize realistic roofs to *natural roofs* induced by bisector graphs of simple polygons: Roughly, we still require a natural roof to drain water but we waive the restriction that every facet of the roof has to be connected to its defining boundary edge. We show how to employ a plane sweep to compute both the minimum-volume and maximum-volume natural roof of a simple polygon with  $n$  vertices in  $\mathcal{O}(n^3 \log n)$  time.

## 2. Preliminaries

### 2.1. Natural roof and bisector graph

Throughout this paper we let  $P$  denote the closure of the area bounded by a simple polygon in the  $xy$ -plane,  $\Pi_0$ , of  $\mathbb{R}^3$ . We denote a plane parallel to  $\Pi_0$  which is at height  $t$  above  $\Pi_0$  by  $\Pi_t$ . As usual, the edges and vertices of the boundary of  $P$  are simply called edges or vertices of  $P$ . A vertex  $v$  of  $P$  is called *reflex* if the interior angle at  $v$  is greater than  $180^\circ$ ; *convex* otherwise. The *interior side*,  $\mathcal{I}(e)$ , of an edge  $e$  of  $P$  is the half-plane within  $\Pi_0$  induced by the supporting line  $\ell(e)$  of  $e$  which locally (close to  $e$ ) overlaps with the interior of  $P$ . The (angular) *bisector* of two different edges  $e_1, e_2$  of  $P$  is the set of all points within  $\mathcal{I}(e_1) \cap \mathcal{I}(e_2)$  that are equidistant from  $\ell(e_1)$  and  $\ell(e_2)$ . (We measure the standard orthogonal distance under the Euclidean metric.) Clearly, if  $e_1$  and  $e_2$  are not parallel to each other then their bisector is a ray that starts at the point of intersection  $\ell(e_1) \cap \ell(e_2)$  and leads into the common interior  $\mathcal{I}(e_1) \cap \mathcal{I}(e_2)$  of  $e_1$  and  $e_2$ . For an edge  $e$  we denote by  $\Pi(e)$  the half-plane induced by the supporting line  $\ell(e)$  of  $e$  that (1) intersects  $\Pi_0$  in  $\ell(e)$ , (2) forms a fixed dihedral angle of  $45^\circ$  with  $\Pi_0$ , and (3) whose projection onto  $\Pi_0$  equals  $\mathcal{I}(e)$ . (We say that  $\Pi(e)$  emanates from  $e$ .) Elementary geometry shows that the bisector of two different edges  $e_1, e_2$  of  $P$  is given by the projection of  $\Pi(e_1) \cap \Pi(e_2)$  onto  $\Pi_0$ . Furthermore, we denote by  $\mathcal{I}(\Pi(e))$  the closed half-space induced by the supporting plane of  $\Pi(e)$  that contains  $\mathcal{I}(e)$ .

**Definition 1 (Roof Model, based on Aichholzer *et al.*<sup>1</sup>).** A roof  $\mathcal{R}(P)$  for a simple polygon  $P$  is the graph of a piecewise-linear continuous function over  $P$  such that

- (1) every facet of  $\mathcal{R}(P)$  is a maximal connected subset of a half-plane  $\Pi(e)$  of some edge  $e$  of  $P$ , and
- (2) the intersection of  $\mathcal{R}(P)$  with  $\Pi_0$  is equal to the boundary of  $P$ .

This definition implies that every roof  $\mathcal{R}(P)$  is a *path-connected* set<sup>a</sup> and forms a terrain over  $P$ . However, it is a special terrain since every facet of  $\mathcal{R}(P)$  is contained in a half-plane that forms a fixed dihedral angle of  $45^\circ$  with  $\Pi_0$ . Hence, two facets of  $\mathcal{R}(P)$  that share an edge form either a vee notch or a wedge, i.e., a portion of the terrain whose form resembles the symbols  $\vee$  and  $\wedge$ . It is natural to regard that side of a facet of  $\mathcal{R}(P)$  which faces  $\Pi_0$  as its interior side. This motivates the following definition.

**Definition 2 (Valley and Ridge).** An edge  $e$  between two neighboring facets of  $\mathcal{R}(P)$  forms a *valley* of  $\mathcal{R}(P)$  if the interior dihedral angle between the facets is greater than  $180^\circ$ . It forms a *ridge* if this angle is less than  $180^\circ$ .

For a real-world roof of a building it would be natural to demand that water will be able to drain off. Aichholzer *et al.*<sup>1</sup> introduce the so-called gradient property to ensure that water will drain off: A facet  $f$  of  $\mathcal{R}(P)$  has the gradient property if, for every point  $p \in f$ , there exists a path on  $\mathcal{R}(P)$  that (i) starts at  $p$ , (ii) follows the steepest gradient, and (iii) reaches the edge  $e$  that defines  $f$ . We consider a less stringent requirement for a roof to drain water: For us it shall suffice that a roof contains no sink, cf. Figs. 3(c) and 3(d).

**Definition 3 (Sink).** Consider a roof  $\mathcal{R}(P)$  of  $P$  and let  $t \in \mathbb{R}^+$ . A portion  $S$  of  $\mathcal{R}(P)$  forms a *sink* of  $\mathcal{R}(P)$  at height  $t$  if (1)  $S$  is a maximal connected component of  $\mathcal{R}(P) \cap \Pi_t$  and (2) there exists  $\varepsilon > 0$  such that all points of  $\mathcal{R}(P) \setminus S$  which are within (Euclidean) distance  $\varepsilon$  of  $S$  have  $z$ -coordinates strictly greater than  $t$ .

**Definition 4 (Natural Roof).** A roof  $\mathcal{R}(P)$  for  $P$  is called a *natural roof* for  $P$  if it does not contain sinks.

The following lemma implies that water does not accumulate anywhere on a roof if and only if it is natural, i.e., does not contain a sink. Hence, roofs without sinks are the “natural” type of roof to study for real-world buildings.

**Lemma 1.** *A roof  $\mathcal{R}(P)$  is a natural roof for  $P$  if and only if the following property holds for all points  $p$  on  $\mathcal{R}(P)$ : There exists a path on  $\mathcal{R}(P)$  from  $p$  to the boundary of  $P$  which is non-increasing, i.e., monotone relative to the  $z$ -coordinate.*

<sup>a</sup>For any two points  $p$  and  $q$  in  $\mathcal{R}(P)$  there exists a path within  $\mathcal{R}(P)$  that links  $p$  to  $q$ .

**Proof.** Obviously, no point of a sink can be linked to the boundary of  $P$  by a  $z$ -monotone path. Thus, if  $\mathcal{R}(P)$  is not a natural roof then the property cannot hold.

Now suppose that  $\mathcal{R}(P)$  is a natural roof for  $P$ , but assume for a contradiction that the claim does not hold for all points on  $\mathcal{R}(P)$ . Let  $t_0 \in \mathbb{R}_0^+$  be the minimum height such that a point  $p$  of  $\mathcal{R}(P) \cap \Pi_{t_0}$  is not linked to the boundary of  $P$  via a monotone path. Since  $\mathcal{R}(P) \cap \Pi_0$  equals the boundary of  $P$ , we have  $t_0 > 0$ . Let  $S$  be the maximal connected component of  $\mathcal{R}(P) \cap \Pi_{t_0}$  that contains  $p$ . Then no point  $q$  of  $S$  can be linked to the boundary of  $P$  via a monotone path; otherwise also a monotone path between  $p$  and the boundary of  $P$  exists via  $q$ . Since  $t_0$  is the smallest  $z$ -coordinate for which this problem occurs,  $S$  has to be a sink, which yields a contradiction to  $\mathcal{R}(P)$  being a natural roof.  $\square$

**Corollary 2.** *Every natural roof of  $P$  drains water.*

**Lemma 3.** *A roof  $\mathcal{R}(P)$  is a natural roof for  $P$  if and only if the following property holds for all values of  $t \in \mathbb{R}$ : The intersection  $\mathcal{C}_t := \mathcal{R}(P) \cap \Pi_t$  does not contain a simple polygon  $P_1$  and another maximal connected component  $S$  such that  $S$  lies completely within the interior of the area bounded by  $P_1$  (in the plane  $\Pi_t$ ).*

**Proof.** The claim is trivially correct if  $\mathcal{C}_t = \emptyset$  and, thus, for all  $t < 0$ . Definition 1 implies that  $\mathcal{C}_0$  equals the boundary of  $P$ , which establishes the claim for  $t = 0$ .

Let  $\mathcal{R}(P)$  be a natural roof for  $P$  and assume that the claim regarding the structure of  $\mathcal{C}_t$  does not hold for some heights  $t \in \mathbb{R}^+$ . Let  $t_0 \in \mathbb{R}^+$  be the smallest height such that this claim does not hold. Then  $\mathcal{C}_{t_0}$  contains a simple polygon  $P_1$  and another maximal connected component  $S$  such that  $S$  lies completely within the interior of the area bounded by  $P_1$ . Since  $S$  is a maximal connected component of  $\mathcal{C}_{t_0}$ , this implies that  $P_1$  and  $S$  belong to two different connected components of  $\mathcal{C}_{t_0}$ . In particular, no point of  $S$  is linked to  $P_1$  via a path within  $\mathcal{C}_{t_0}$ . Let  $p$  be a point of  $S$ . Any path on  $\mathcal{R}(P)$  from  $p$  to the boundary of  $P$  must cross  $P_1$ . Since  $p$  and  $P_1$  are at the same height  $t_0$  but within different connected components of  $\mathcal{C}_{t_0}$ , this path cannot be monotone relative to the  $z$ -coordinate, which contradicts Lemma 1.

Now consider a roof  $\mathcal{R}(P)$  and assume that the claim regarding the structure of  $\mathcal{C}_t$  holds for all heights  $t$ , but that  $\mathcal{R}(P)$  is not a natural roof. Hence,  $\mathcal{R}(P)$  has at least one sink. Let  $t_0$  be the smallest height at which a sink occurs, and let  $S$  be a sink at height  $t_0$ . Since  $\mathcal{R}(P)$  does not contain a horizontal facet,  $S$  is given by a collection of line segments that form a planar straight-line graph (PSLG). Furthermore, if one point out of the relative interior of an edge of  $\mathcal{R}(P)$  belongs to  $S$  then the entire edge belongs to  $S$ , including its two endpoints. That is,  $S$  is formed by a set of connected edges of  $\mathcal{R}(P)$ . We now study the (orthogonal) projection of  $\mathcal{R}(P)$  onto  $\Pi_0$ . Consider all facets of  $\mathcal{R}(P)$  that are incident to edges of  $S$  and whose projection onto  $\Pi_0$  lies within the outer face of (the projection of)  $S$ . Let  $t_1$  be the minimum  $z$ -coordinate of the vertices of these facets, excluding the vertices of  $S$ . We have  $t_1 > t_0$ . Then  $\Pi_{t_1}$  intersects all these facets of  $\mathcal{R}(P)$  in a polygon  $P_1$ . The projection of  $P_1$  onto  $\Pi_0$  bounds a polygonal area  $A_1$  that contains the projection

of  $S$  in its interior. The continuity of  $\mathcal{R}(P)$  implies that every path on  $\mathcal{R}(P)$  which leads from a point of  $P_1$  to the boundary of  $P$  has to pass through at least one point of  $\mathcal{R}(P)$  which is at height  $t_0$  and whose projection onto  $\Pi_0$  does not fall into  $A_1$ . Hence,  $\mathcal{R}(P)$  contains a polygon  $P_2$  at height  $t_0$  such that the projections of  $P_2$ ,  $P_1$  and  $S$  onto  $\Pi_0$  are nested. This implies that  $S$  lies within the interior of the region of  $\Pi_{t_0}$  bounded by  $P_2$ , which yields a contradiction to our assumption regarding the structure of  $\mathcal{C}_t$  for all heights  $t$ .  $\square$

Ridges allow an alternative characterization of natural roofs:

**Lemma 4.** *Let  $G$  be the straight-line subgraph of  $\mathcal{R}(P)$  given by all of edges of a roof  $\mathcal{R}(P)$  that form ridges. Then, the roof  $\mathcal{R}(P)$  is a natural roof for  $P$  if and only if  $G$  does not contain a cycle.*

**Proof.** The claim is readily proved by resorting to Lemma 3 and understanding that a polygon  $P_1$  contains another maximal connected component  $S$  of  $\mathcal{C}_t := \mathcal{R}(P) \cap \Pi_t$  if and only if a ridge cycle  $C$  exists among the edges of  $\mathcal{R}(P)$  such that the projection of  $C$  onto  $\Pi_t$  separates  $P_1$  from  $S$ .  $\square$

**Definition 5 (Bisector Graph<sup>1</sup>).** A connected planar straight-line graph is a *bisector graph*,  $\mathcal{B}(P)$ , of  $P$  if

- (1) all its edges are portions of bisectors of edges of  $P$ ,
- (2) it has no degree-two node, and
- (3) there exists a geometric cover and bijection between its degree-one nodes and the input vertices of  $P$ : each degree-one node coincides (as a point) with exactly one input vertex.

The straight skeleton of  $P$  is known to be one specific bisector graph of  $P$ .<sup>1</sup> In general, a simple polygon will admit several different bisector graphs. In Fig. 1, we see two bisector graphs of a simple polygon.

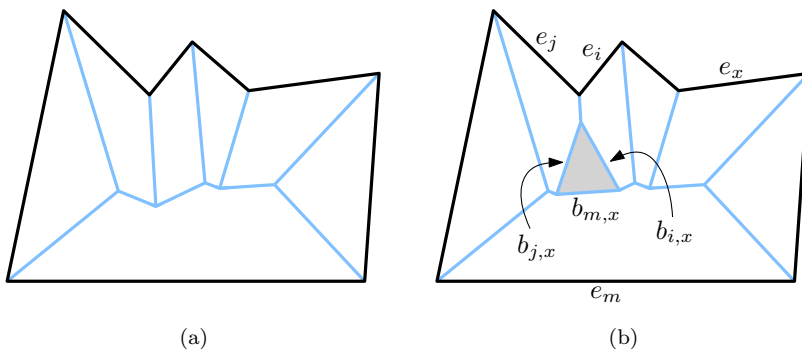


Fig. 1. (a) A polygon  $P$  and its straight skeleton. (b) Another bisector graph of  $P$ , where the facet shaded in gray is not connected to the boundary edge  $e_x$  of  $P$ . We write  $b_{i,j}$  for the bisector between the edges  $e_i$  and  $e_j$ .

In order to distinguish between the elements of the boundary of  $P$  and of a bisector graph we call the edges of a bisector graph *arcs*. Common end-points of arcs are called *nodes*. For an edge  $e$  of  $P$  we say that the *edge  $e$  defines a facet  $f$*  of  $\mathcal{R}(P)$  if  $f$  is contained in  $\Pi(e)$ . Note that some edges may define multiple facets; cf. Fig. 1(b) where the facet shaded in gray is also contained in  $\Pi(e)$ . This figure can be interpreted as a bisector graph or as the projection of a roof onto  $\Pi_0$ . Indeed, there is a bijection between roofs and bisector graphs:

**Theorem 5 (Roof  $\leftrightarrow$  Bisector Graph<sup>1</sup>).** *Every roof for  $P$  corresponds to a unique bisector graph of  $P$ , and vice versa.*

**Definition 6 (Roof Volume).** *The volume of a roof  $\mathcal{R}(P)$  is the volume of the three-dimensional polyhedral shape bounded by  $\mathcal{R}(P)$  and  $\Pi_0$ .*

## 2.2. Motivation

The roof defined by the straight skeleton of  $P$  need neither minimize nor maximize the roof volume among all roofs over  $P$  that exhibit the (natural) gradient property.<sup>1</sup> Rather, as Fig. 2 shows, the bisector graphs that correspond to minimum-volume and maximum-volume roofs may differ from the straight skeleton: Fig. 2(a) shows the straight skeleton of a simple polygon. In Fig. 2(b), we see another bisector graph of the same polygon, where the disconnected facets shaded in light blue allow for a larger roof volume. Both facets lie in the half-plane  $\Pi(e)$  of the input edge  $e$  of  $P$ . The bisector graph that corresponds to the minimum-volume roof, shown in Fig. 2(c), differs substantially from both the straight skeleton and the maximum-volume roof of  $P$ . (The bisector graphs of the minimum-volume roof and maximum-volume roof

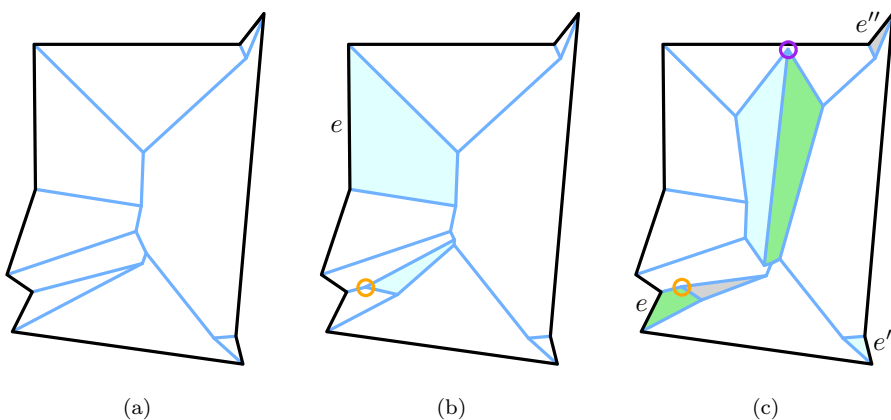


Fig. 2. In (a), we see the straight skeleton of  $P$ , in (b) the bisector graph of the maximum-volume natural roof of  $P$ , and in (c) the bisector graph of the minimum-volume natural roof. Areas with a common color belong to the same input edge, i.e., lie in the same respective half-plane (color online).

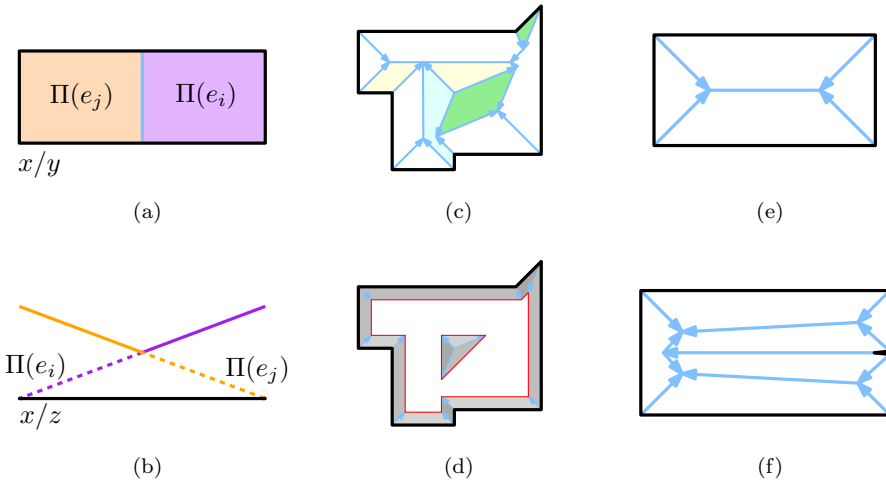


Fig. 3. In (a) and (b), we see a rectangle and the upper envelope of the planes emanating from its input edges. In (c), we see a polygon where the lower envelope creates a sink; a horizontal cut through the roof by a plane at a particular height is shown in red in (d). In (e) and (f), we see two polygons where the polygon in (f) clearly has a larger area (and contains the polygon in (e)) but its skeleton-induced roof has a smaller volume than the roof of (e) (color online).

were computed by our own sample implementation of our algorithm; see Sec. 8 for details.)

It is also worthwhile to note that several “obvious” approaches to minimizing or maximizing the roof volume do not work. For instance, computing the lower or upper envelope of the half-planes  $\Pi(e)$  for all edges  $e$  of  $P$  need not yield a (natural) roof: The upper envelope does not even create a roof, as we can see in Figs. 3(a) and 3(b). A similar problem occurs for the lower envelope of all half-planes which also does not create a roof. (The intersection of the lower envelope with  $\Pi_0$  is not restricted to the boundary of  $P$ .) A natural refinement of this idea might be to consider the arrangement of all half-planes  $\Pi(e)$  of all edges  $e$  of  $P$ , and to discard all those facets (within that arrangement) of a half-plane  $\Pi(e)$  that intersect  $\Pi_0$  outside of  $e$ . Still, the lower envelope of those portions of the half-planes may contain sinks; see Figs. 3(c) and 3(d). As a result water will not drain to the outside and therefore it is not a natural roof.

We also note that a containment relation among polygons need not translate to a containment relation among the roofs induced by their straight skeletons: As shown in Figs. 3(e) and 3(f), a polygon  $P$  can be contained in a polygon  $P'$  (and, thus, have a smaller area than  $P'$ ), but the volume of the only natural roof of  $P$  may still be greater than the volume of the only natural roof of  $P'$ .

It is easy to understand that the lower envelope of two natural roofs may contain a sink that prevents water from draining. However, the same problem may also arise for upper envelopes: The upper envelope of two natural roofs need not be a natural roof either, as we can see in Fig. 4.

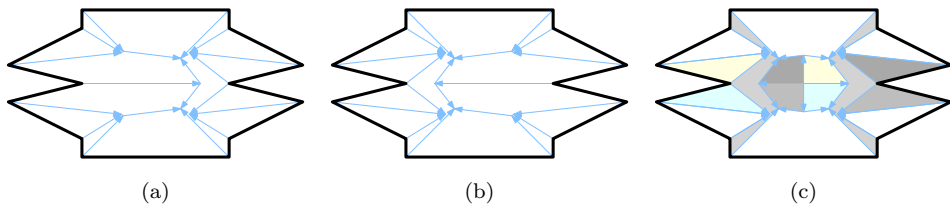


Fig. 4. In (a) and (b), we see two different natural roofs, and in (c) we see the upper envelope of these two roofs which contains a sink (above the center of symmetry of the polygon).

### 3. Characterization of Minimum-/Maximum-Volume Roofs

We proceed with a characterization of minimum-volume and maximum-volume natural roofs. In Sec. 4 we will explain how we can exploit this characterization and compute such roofs. For the sake of (mostly descriptive) simplicity we assume that  $P$  is in general position:

- No two edges of  $P$  shall be parallel to each other.
- No four half-planes, emanating from the edges of  $P$ , shall meet in a common point.

The second assumption implies that there is no circle such that four or more supporting lines of edges of  $P$  are tangent to it. Later on we will waive these restrictions and discuss the general case in Sec. 5. We note that a roof for a polygon can contain a horizontal edge only if two edges of the polygon are parallel. Since our general-position assumption rules out horizontal edges of  $\mathcal{R}(P)$ , the existence of a monotone path from a point  $p$  on  $\mathcal{R}(P)$  to the boundary of  $P$  implies the existence of a strictly monotone path. Similarly, for our simplified setting, if we regard a single vertex as a degenerate polygon then every non-empty intersection  $\mathcal{R}(P) \cap \Pi_t$  is given by a collection of simple polygons rather than arbitrary PSLGs. In particular, every sink of  $\mathcal{R}(P)$  consists of just one vertex of  $\mathcal{R}(P)$  and cannot include edges of  $\mathcal{R}(P)$ .

**Definition 7 (Arrangement  $\mathcal{A}^c(P)$ ).** We denote the arrangement induced by all half-planes emanating from edges of  $P$  by  $\mathcal{A}^c(P)$ .

The arrangement  $\mathcal{A}^c(P)$  partitions the space  $\mathbb{R}^3$  into convex polytopes. We call one facet of such a polytope an *arrangement facet*. Since all natural roofs are formed by portions of half-planes emanating from edges of  $P$ , a facet of a roof (called *roof facet* in the sequel) is formed by a non-empty set of adjacent arrangement facets (which all lie within the same half-plane  $\Pi(e)$  for some edge  $e$  of  $P$ ):

**Lemma 6.** *Every edge of  $\mathcal{R}(P)$  is formed by the union of some edges of  $\mathcal{A}^c(P)$  and every roof facet of  $\mathcal{R}(P)$  is formed by the union of a non-empty set of arrangement facets of  $\mathcal{A}^c(P)$ .*

**Proof.** Consider a roof  $\mathcal{R}(P)$  of  $P$ . Every roof facet of  $\mathcal{R}(P)$  is contained in exactly one half-plane defined by an edge of  $P$ , and every boundary edge of a roof facet is

either an edge of  $P$  or is formed by the intersection of two such half-planes of  $P$ . Now recall that the arrangement  $\mathcal{A}^C(P)$  is induced by the half-planes of all edges of  $P$ , thereby concluding the proof.  $\square$

**Corollary 7.** *Every roof for  $P$  consists only of arrangement facets of  $\mathcal{A}^C(P)$ .*

We now turn our attention to the computation of bisector graphs. Wavefront propagation<sup>1,7</sup> is a well-known strategy for computing straight skeletons. It is a shrinking process in which every boundary edge of  $P$  is offset inwards in a self-parallel manner. Initially, the segments of the wavefront correspond to the boundary edges of the polygon. During the wavefront propagation every wavefront segment moves at unit speed towards the interior of  $P$ . After the propagation has finished every point in  $P$  has been swept by the wavefront exactly once. We follow a common notion and regard the wavefront as a function of time  $t$ , and write  $\mathcal{W}_P(t)$  to denote the shrinking (wavefront) polygons at time  $t$ . At time  $t$  every wavefront segment is at distance  $t$  from its input edge. Thus, every wavefront segment lies in the offset of the supporting line of its defining input edge. We define the supporting line of the offset of the edge  $e$  of  $P$  at time  $t$  as  $o(e, t) := \ell(e) + t \cdot n_e$ , where  $n_e$  is the inward unit normal vector and  $\ell(e)$  is the supporting line of  $e$ , and call it *offset supporting line* of  $e$  at time  $t$ . Furthermore, the interior side of such a supporting line is defined as the half-plane within  $\Pi_0$  induced by the offset supporting line which is a subset of  $\mathcal{I}(e)$ .

As time progresses, the normal distance of each wavefront segment to its defining input edge grows. The points of intersection between consecutive wavefront segments lie on the bisectors of their defining input edges. The wavefront vertices move along these bisectors and trace out the arcs of a bisector graph. A reflex (convex) vertex of  $P$  becomes a reflex (convex, resp.) wavefront vertex. For straight skeletons two types of events occur during the wavefront propagation: *edge events* and *split events*.<sup>7</sup> These events are *mandatory* in the sense that at the event time the combinatorial structure of the wavefront  $\mathcal{W}_P(t)$  has to be modified in order to maintain weak planarity<sup>b</sup> of  $\mathcal{W}_P(t)$ .

**Definition 8 (Edge Event<sup>1</sup>).** An *edge event* occurs when a wavefront edge shrinks to length zero.

At the time of an edge event the zero-length edge of the wavefront is removed and its two neighboring edges become adjacent.

**Definition 9 (Split Event<sup>1</sup>).** A *split event* occurs when a reflex wavefront vertex intersects a wavefront edge.

<sup>b</sup>A polygon is weakly planar (or weakly simple) if it is the boundary of a region that is topologically equivalent to a disk; (portions of) edges may overlap and vertices may coincide.

The intersected wavefront edge is split at the point of intersection. New adjacencies occur between the edge split and each of the two edges incident to the reflex vertex.

During the wavefront propagation the area contained in the interior of the wavefront polygons shrinks monotonically. This property still holds at times where the combinatorial structure of the wavefront changes due to edge or split events.

The standard wavefront propagation, with all edge and split events handled properly, traces out the straight skeleton of the input polygon. Since we are interested in computing other bisector graphs, too, we consider additional events. In the sequel we will introduce two new event types which we call *create event* and *vertex event*. As changing the combinatorics of the wavefront requires the intersection of at least three offset supporting lines but our general-position assumption rules out an intersection among more than three offset supporting lines, we can deduce Lemma 8.

**Lemma 8.** *Every wavefront event occurs at the common intersection point of exactly three offset supporting lines of  $P$ .*

Of course, we are primarily interested in only those intersections of three offset supporting lines which do not destroy basic properties of the wavefront. Such events are called admissible wavefront events:

**Definition 10 (Admissible Wavefront Event).** An intersection of three offset supporting lines at time  $t$  is called an *admissible wavefront event* if the point  $p$  of intersection lies on at least one wavefront edge of  $\mathcal{W}_P(t)$ , and if it is possible to modify  $\mathcal{W}_P(t)$  locally around  $p$  such that, for every sufficiently small  $\varepsilon \in \mathbb{R}^+$ , the modified wavefront  $\mathcal{W}_P(t + \varepsilon)$  is planar and strictly contained within the interior of the area bounded by  $\mathcal{W}_P(t)$ .

The first condition of Definition 10 rules out the creation of new wavefront loops inside or outside of the current wavefront. The two other conditions are required for being able to continue the wavefront propagation after an event such that the planarity of the wavefront is maintained and such that it keeps moving inwards. Of course, several admissible wavefront events may happen at the same time. However, due to our general-position assumption they do not interfere with each other and, thus, can be handled in arbitrary order and individually.

In the sequel we explain all admissible wavefront events in more detail. In order to make sure that all possible interactions are covered without having to resort to clumsy mathematical arguments we start with a systematic classification of all possible intersections of wavefront edges and their offset supporting lines.

Without loss of generality we consider one wavefront edge as well as the movement direction (i.e., the interior side) of its offset supporting line as fixed. Then the possible scenarios can be arranged in a matrix, where the rows correspond to all five possible positions of a second wavefront edge (if it exists), and the columns circle through the four combinations of movement directions of the remaining two offset

supporting lines. These movement directions are indicated by small black arrows in Figs. 5 to 8. If the scenario represents an admissible wavefront event then the wavefront at the event time is drawn in black and the new wavefront is drawn in green. Where helpful, magenta lines illustrate the wavefront prior to the event. If a scenario is not possible due to inconsistent interior sides of the offset supporting lines then the wavefront is drawn in red. The bisectors are drawn in blue. We use dotted gray lines for the offset supporting lines after the event, and dashed gray for all other offset supporting lines. All possible combinatorial scenarios for one, two, three, four or six wavefront elements on three offset supporting lines are illustrated in Figs. 5 to 8. Note that at most six wavefront elements can be defined around the common intersection of three offset supporting lines. Furthermore, we can not place five wavefront elements incident at a common point such that they have a consistent interior.

It comes as no surprise that our classifications contain also the standard edge and split events. Figures 6(m), 6(n) and 6(r) show all possible scenarios for an edge event. Of course, two edge events may also coincide; see Fig. 6(i). An edge event where all three incident wavefront edges shrink to zero length is a trivial wavefront event since after the event the respective wavefront component has vanished. That is, one component of the wavefront collapses to a point; see Figs. 6(d), 6(h), 6(p) and 6(t). Similarly, a split event is shown in Fig. 7(t).

We now turn our focus on wavefront events that involve one or two wavefront edges. Figure 5(i) shows the only possible scenario for one wavefront edge, while all three possible scenarios that involve two wavefront edges are shown in Figs. 5(c), 5(e) and 5(g). (Several other scenarios are possible for two wavefront edges, but in all these cases the combinatorics of the wavefront do not change after the event; see Fig. 7.)

**Definition 11 (Create Event).** A wavefront event at a point  $p$  of the wavefront is a *create event* if one or two wavefront edges are incident at  $p$  and if the wavefront can be modified at  $p$  by introducing a new wavefront edge, as illustrated in Fig. 5(i) (for one incident wavefront edge) and Figs. 5(c), 5(e) and 5(g) (for two incident wavefront edges).

We note that all new wavefront vertices move along bisectors (shown as blue arrows in Fig. 5). A create event is *optional* as it can be used to modify the combinatorial structure of the wavefront during the propagation. However, this modification is not required to maintain the weak planarity of the propagating wavefront. There are two scenarios under which a create event can occur. The first scenario occurs if differences in speed cause an offset supporting line of an edge of  $P$  to overtake or to be overtaken by a reflex wavefront vertex; cf. Figs. 5(c), 5(e) and 5(g). The second one occurs if two offset supporting lines of edges of  $P$  become incident in a common point on a wavefront edge; cf. Fig. 5(i). Note that an edge event can occur at the same point as a create event. However, they can be processed without complication one after the other. We illustrate both create event scenarios in Fig. 2: The orange

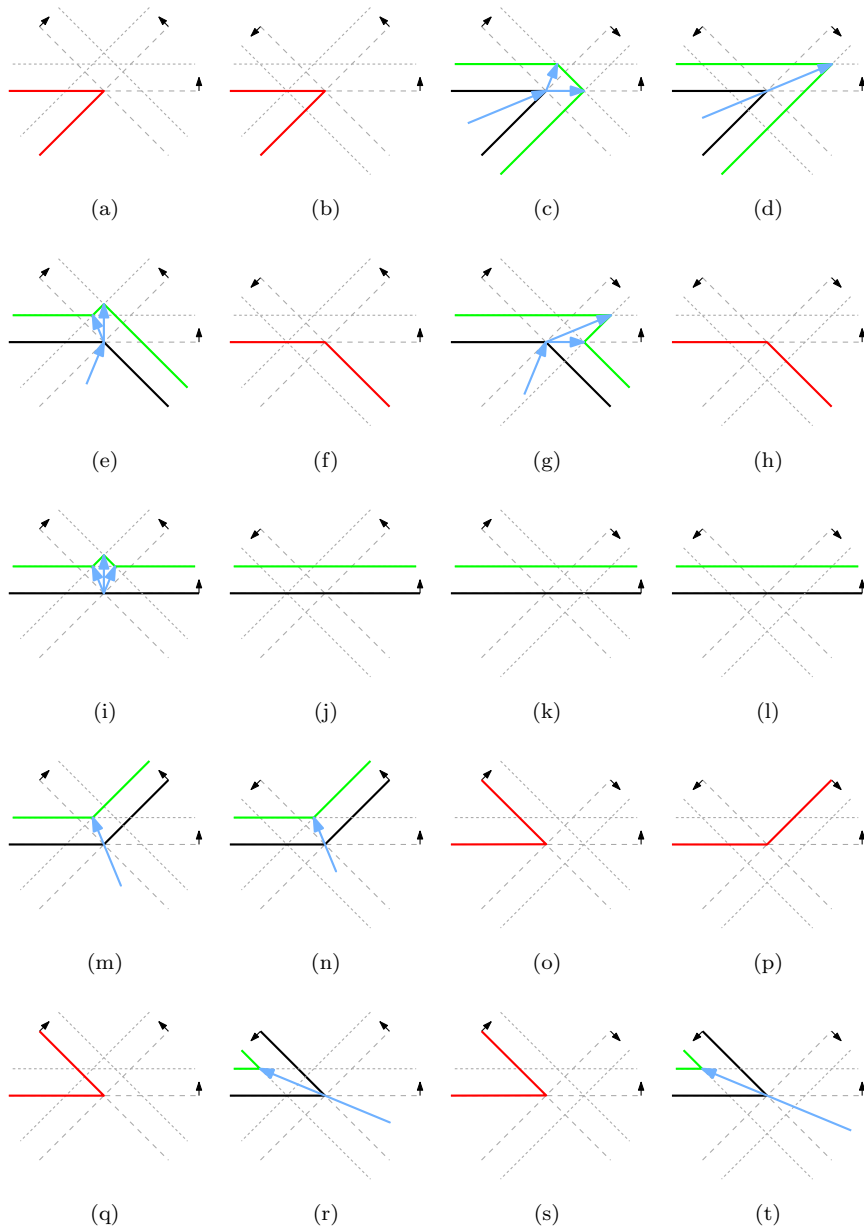


Fig. 5. Three offset supporting lines meet at a point  $p$ . We see all possible combinatorial scenarios if up to two wavefront edges are incident at  $p$  (color online).

circles in Figs. 2(b) and 2(c) mark the first scenario and the purple circle in Fig. 2(c) marks the second one.

If four wavefront edges intersect at a point  $p$  then only one scenario is possible in addition to the standard split event, see Fig. 7(d). Similarly, for six wavefront

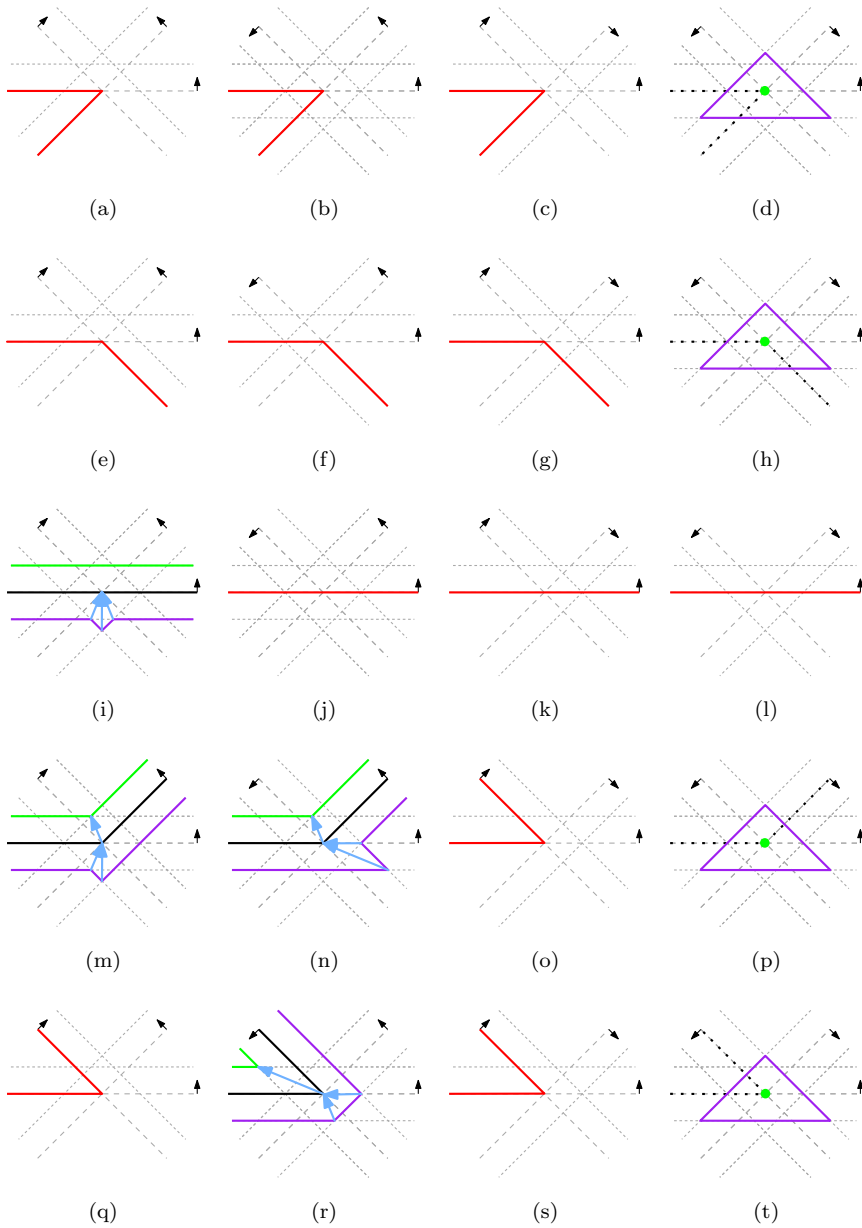


Fig. 6. Three offset supporting lines meet at a point  $p$ . We see all possible combinatorial scenarios if three wavefront edges are incident at  $p$  (color online).

edges only the scenario of Fig. 8(d) is possible. These two scenarios correspond to our new vertex event:

**Definition 12 (Vertex Event).** A wavefront event at a point  $p$  of the wavefront is a *vertex event* if four or six wavefront edges meet at  $p$  such that it is not a split

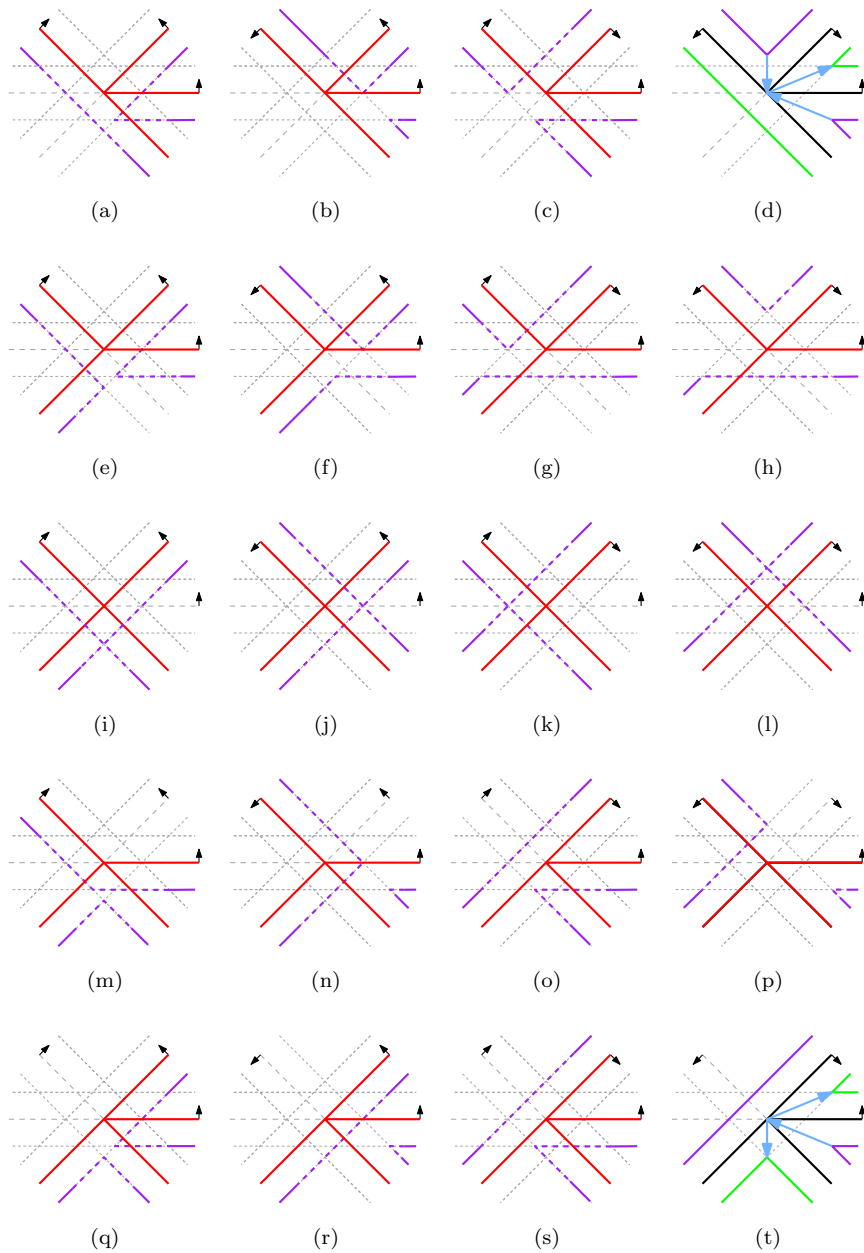


Fig. 7. Three offset supporting lines meet at a point  $p$ . We see all possible combinatorial scenarios if four wavefront edges are incident at  $p$ . For each scenario that does not correspond to an admissible event we show a non-intersecting wavefront pairing illustrated by wavefront edges either before or after the event (in dashed magenta) (color online).

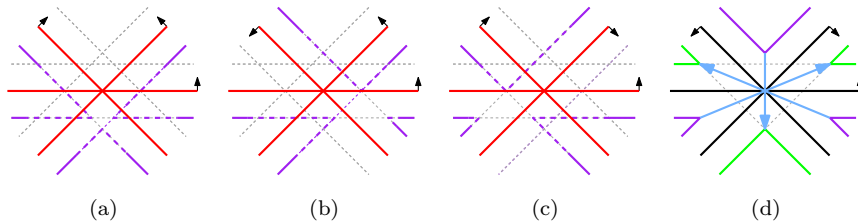


Fig. 8. Three offset supporting lines meet at a point  $p$ . We see all possible combinatorial scenarios if six wavefront edges are incident at  $p$  (color online).

event and such that the wavefront can be modified as in Fig. 7(d) (for four incident wavefront edges) or in Fig. 8(d) (for six incident wavefront edges).

Again, all new wavefront vertices move along bisectors. A vertex event is well-known in the context of straight skeleton computation.<sup>3</sup> Due to our general-position assumption this standard vertex event cannot occur. However, a vertex event can occur also for input in general position after a create event took place. Every vertex event is mandatory and occurs, in general position, only after the occurrence of a create event. In general position we only have three offset supporting lines intersecting in a common point. Thus, all incident collinear wavefront edges have to lie on the same offset supporting line. These collinear edges can only appear due to a create event.

Figures 7 and 8 immediately tell us that every vertex event involves exactly two or exactly three reflex wavefront vertices. Furthermore, after the event one (three, resp.) convex wavefront vertices remain.

**Lemma 9.** *Let  $v$  be a wavefront vertex at the point  $p$  of a create event. Then  $v$  is a reflex vertex.*

**Proof.** If  $v$  is convex then we cannot add a new edge; cf. Fig. 5. □

**Lemma 10.** *Let a create event occur at a point  $p$  such that exactly one wavefront edge is incident. Then, the two edges  $e_1$  and  $e_2$  added due to the create event are incident at a common reflex wavefront vertex  $v$ .*

**Proof.** Figure 5(i) is the only possible scenario in this case. □

Several approaches<sup>1,3,7</sup> to handling edge and split events during the standard wavefront propagation are known. Our new events also take place on the wavefront at the intersection of three offset supporting lines in a common point. Thus, any of these approaches is also applicable to our more general setting. Once we are given an event, we can easily check whether it is an admissible wavefront event and modify the wavefront accordingly, as illustrated in Figs. 5 to 8.

Let  $p$  be a point where an admissible wavefront event takes place at time  $t$ . Then some edges were traced out by wavefront vertices until they reached  $p$  at time  $t$ ,

and some other edges may start at time  $t$  from  $p$ . The wavefront vertices that trace out the edges until  $t$  are, perceived from the viewpoint of  $p$ , *incoming* wavefront vertices, and *outgoing* otherwise.

**Lemma 11.** *No event replaces an incoming convex wavefront vertex by an outgoing reflex wavefront vertex, and all events except for the create event replace incoming reflex wavefront vertices by outgoing convex wavefront vertices.*

**Proof.** This claim is readily established by taking a look at Figs. 5 to 8.  $\square$

In the sequel we study a wavefront propagation that is extended to handle all edge, split and vertex events if and when they occur. Create events can be handled but may also be ignored. (We will later on investigate which create events we will want to handle.) From this point on we refer to this extended wavefront propagation simply by wavefront propagation.

**Lemma 12.** *Every facet traced out during a wavefront propagation by portions of an offset supporting line of  $P$  forms a simple polygon without holes.*

**Proof.** Every facet of the straight skeleton of  $P$  is a simple polygon that is monotone with respect to the supporting line of its defining input edge.<sup>1</sup> In particular, split events do not cause faces with holes. The fact that the wavefront moves inwards and that all mandatory events are handled implies that every facet  $f$  generated by our wavefront propagation is bounded by simple polygons. We will now verify that no hole can be created in  $f$  during a wavefront propagation.

Let edge  $e$  of  $P$  define  $f$ . We assume that  $f$  contains a hole, then a wavefront edge defined by  $e$  is split by a create event (Fig. 5(i)) into two new wavefront edges, and these two edges merge again later on. This merge could only happen due to a vertex event (Fig. 7(d)), but such an event requires two incoming reflex wavefront vertices while that create event sends out only one reflex wavefront vertex. Lemma 11 tells us that convex wavefront vertices do not turn into reflex wavefront vertices, thus we arrive at a contradiction.

Note that Fig. 5(c) shows a create event that sends out two reflex vertices, but that event occurs at a wavefront vertex and does not split a wavefront edge. Hence, the two wavefront edges lie on different half-planes and cannot bound a single facet.  $\square$

**Lemma 13.** *Every wavefront propagation over  $P$  traces out a path-connected structure in  $\Pi_0$ .*

**Proof.** Let  $\mathcal{G}$  be the structure, within  $\Pi_0$ , traced out by the vertices of a wavefront propagation over  $P$ . Observe that  $\mathcal{G}$  forms a PSLG because all wavefront vertices move along straight-line paths. For  $t \in \mathbb{R}_0^+$  we let  $\mathcal{G}_t$  denote the structure traced out by  $\mathcal{W}_P(t)$  until time  $t$ . We start with proving that  $\mathcal{G}_{t_1} \cup \mathcal{W}_P(t_1)$  is path-connected for all  $t_1 \geq t_0$  if  $\mathcal{G}_{t_0} \cup \mathcal{W}_P(t_0)$  is path-connected, for all  $t_0 \in \mathbb{R}^+$ .

Let  $t_0, t_1 \in \mathbb{R}_0^+$  be arbitrary but fixed, with  $t_1 > t_0$ . Assume that  $\mathcal{G}_{t_0} \cup \mathcal{W}_P(t_0)$  is connected. The claim is trivial if no event occurs strictly before time  $t_1$  and at or after time  $t_0$ . So suppose that one event occurs within this (half-open) time interval. Without loss of generality, we assume that the event occurs right at time  $t_0$ . Let  $p$  be the point at which the event occurs. An inspection of Figs. 5 to 8 shows that the vertex event of Fig. 7(d) is the only event in which a wavefront is split and one wavefront polygon  $Q$  is not connected directly to  $\mathcal{G}_{t_1}$  by a new arc. In all other cases, all new arcs of  $\mathcal{G}_{t_1}$  are connected to a node of  $\mathcal{G}_{t_1}$  at  $p$ , and all polygons of  $\mathcal{W}_P(t_1)$  remain connected to  $\mathcal{G}_{t_1}$  via newly created arcs. Let  $v$  be the node of  $\mathcal{G}_{t_0}$  at  $p$ . We note that the two wavefront edges that merged in the course of this vertex event (Fig. 7(d)) are contained in a common offset supporting line,  $o(e, t_0)$ , of some edge  $e$ . Lemma 12 tells us that the area swept by  $o(e, t)$  forms a simple polygon: It is bound by a polygon  $Q'$  formed by  $\mathcal{G}_t(P)$ ,  $\mathcal{W}_P(t)$ , and (possibly) by  $e$ . Furthermore,  $Q'$  has  $v$  on its boundary for all  $t \geq t_0$ . Hence, it suffices to walk along  $Q'$  to find a path that connects  $v$  with the new wavefront polygon  $Q$  of  $\mathcal{W}_P(t_1)$ .

Induction on the number of events establishes the claim if more than one event occurs between the times  $t_0$  and  $t_1$ .

All points of  $\mathcal{G}_{t_0} \cup \mathcal{W}_P(t_0)$  are connected for  $t_0 = 0$  because  $\mathcal{W}_P(0)$  equals the boundary of  $P$ . Since  $\mathcal{W}_P(t)$  has vanished for all sufficiently large values of  $t$  (after the time of the last event), and  $\mathcal{G} = \mathcal{G}_t$  for all such values of  $t$ , we conclude that  $\mathcal{G}$  is path-connected. □

**Lemma 14.** *Every wavefront propagation over  $P$  traces out a bisector graph of  $P$ .*

**Proof.** Let  $\mathcal{G}$  be the structure traced out by a wavefront propagation over  $P$ . In the sequel we show that all conditions of Definition 5 hold for  $\mathcal{G}$ . At  $t = 0$  the wavefront  $\mathcal{W}_P(t)$  is equal to the boundary of  $P$ . By definition, every input vertex of  $P$  corresponds to a wavefront vertex that moves inwards and traces out an arc. Thus, every input vertex of  $P$  corresponds to a node of degree one in  $\mathcal{G}$ .

The definition of the initial movement of the wavefront vertices and the handling of the events implies that every wavefront vertex moves along a bisector of edges of  $P$ . Therefore,  $\mathcal{G}$  consists of portions of bisectors of  $P$ .

Every admissible wavefront event results in a change of the combinatorial structure of the wavefront. As we have no event that produces a degree-one or degree-two node, every node of  $\mathcal{G}$  (except for the nodes that correspond to input vertices of  $P$ ) is of degree at least three.

The weak planarity of the wavefront at any time and the fact that every point within the interior of  $P$  is traversed exactly once by the wavefront guarantees that  $\mathcal{G}$  is planar. The connectedness of  $\mathcal{G}$  was established in Lemma 13, thus concluding the proof. □

**Lemma 15.** *Every wavefront propagation over  $P$  results in a natural roof over  $P$ .*

**Proof.** Theorem 5 and Lemma 14 imply that every wavefront propagation results in a roof  $\mathcal{R}(P)$  for  $P$ . The projection of  $\mathcal{C}_t := \mathcal{R}(P) \cap \Pi_t$  onto  $\Pi_0$  matches  $\mathcal{W}_P(t)$  for every  $t \in \mathbb{R}$ . Since  $\mathcal{W}_P(t)$  does not contain nested polygons, Lemma 3 establishes the claim.  $\square$

**Lemma 16.** *Every natural roof over  $P$  corresponds to a wavefront propagation of  $P$ .*

**Proof.** Let  $\mathcal{R}(P)$  be a natural roof over  $P$  and let  $\mathcal{B}(P)$  be the bisector graph that corresponds to  $\mathcal{R}(P)$ . Initially the wavefront vertices move along the arcs of  $\mathcal{B}(P)$ . The node  $p$  of  $\mathcal{B}(P)$  that is the first to be reached by the wavefront at time  $t_0$  corresponds to the lowest vertex (with non-zero  $z$ -coordinate) of  $\mathcal{R}(P)$ . Since all vertices of  $\mathcal{R}(P)$  that are adjacent to  $p$  have greater  $z$ -coordinates than  $p$ , the projections of the corresponding edges of  $\mathcal{R}(P)$  form bisector rays that point (locally) to the interior of the wavefront  $\mathcal{W}_P(t_0)$ . Since the wavefront propagation can choose among any of the geometrically possible ways to modify the wavefront at  $p$ , it can also reproduce the new arcs of  $\mathcal{B}(P)$  at  $p$ . (Recall Figs. 5–8.) Induction on the ordered sequence of nodes of  $\mathcal{B}(P)$  completes the proof.  $\square$

**Corollary 17.** *There is a bijection between the set of natural roofs over  $P$  and the set of wavefront propagations within  $P$ .*

**Definition 13 (Natural Arrangement  $\mathcal{A}(P)$ ).** A facet of the arrangement  $\mathcal{A}^c(P)$  is said to be traversed by a wavefront propagation if it belongs to a facet of the natural roof which corresponds to that wavefront propagation. The collection of all arrangement facets traversed by all wavefront propagations is called *natural arrangement*  $\mathcal{A}(P)$ .

**Corollary 18.** *Every facet of  $\mathcal{A}(P)$  is contained in a natural roof over  $P$ , and every natural roof over  $P$  is formed by a union of facets of  $\mathcal{A}(P)$ .*

**Lemma 19.** *The lower envelope  $\mathcal{E}_\ell$  of  $\mathcal{A}(P)$  is a natural roof over  $P$ .*

**Proof.** Every natural roof over  $P$  is contained in  $\mathcal{A}(P)$ . The intersection of every natural roof and  $\Pi_0$  is equal to the boundary of  $P$ . Thus,  $\mathcal{E}_\ell \cap \Pi_0$  is equal to the boundary of  $P$ , too. Every roof is a piecewise linear continuous function over  $P$ . Therefore, also the lower envelope over this set of functions is piecewise linear, continuous, and defined over  $P$ . Since every facet of  $\mathcal{E}_\ell$  is contained in a half-plane  $\Pi(e)$  for some edge  $e$  of the boundary of  $P$ ,  $\mathcal{E}_\ell$  forms a roof over  $P$ .

Suppose that  $\mathcal{E}_\ell$  is not a natural roof. Then there exists at least one point that is not linked to the boundary of  $P$  by a strictly  $z$ -monotone path. Let  $p$  be a point of minimal  $z$ -coordinate among those points. We recall that no facet or edge of  $\mathcal{E}_\ell$  lies in a plane parallel to  $\Pi_0$ . Thus, a point in the interior of such a facet or edge can be linked via a strictly  $z$ -monotone path to a respective boundary vertex of the

face or edge. Hence,  $p$  has to be a vertex of  $\mathcal{E}_\ell$ . Our assumption on  $p$  implies that all vertices adjacent to  $p$  in  $\mathcal{E}_\ell$  have a greater  $z$ -coordinate than  $p$ . However,  $p$  also has to be a vertex of at least one natural roof over  $P$ : Every facet of  $\mathcal{E}_\ell$  is part of at least one natural roof over  $P$ , as implied by Corollary 18. Since no natural roof contains a sink, no such point  $p$  can exist and we arrive at a contradiction. Therefore we conclude that  $\mathcal{E}_\ell$  is a natural roof over  $P$ .  $\square$

**Corollary 20.** *The lower envelope  $\mathcal{E}_\ell$  of  $\mathcal{A}(P)$  is the minimum-volume natural roof over  $P$ .*

**Corollary 21.** *The minimum-volume natural roof over  $P$  also is a natural roof of minimum height over  $P$ .*

Note that the minimum-volume roof need not always be a natural roof: In Fig. 3(c) we see a structure that clearly has less volume than the roof induced by the classic straight skeleton, which for that polygon is the minimum-volume natural roof.

**Lemma 22.** *The upper envelope  $\mathcal{E}_u$  of  $\mathcal{A}(P)$  is a natural roof over  $P$ .*

**Proof.** The same arguments as used in the proof of Lemma 19 establish the fact that  $\mathcal{E}_u$  is a roof over  $P$ . We use the characterization of Lemma 4 to prove that  $\mathcal{E}_u$  is a natural roof.

Suppose  $\mathcal{E}_u$  is not a natural roof, in particular that  $\mathcal{E}_u$  contains a cycle of ridge edges. We project all ridge edges of  $\mathcal{E}_u$  onto  $\Pi_0$ . The union of these projected edges partitions  $\Pi_0$  into one unbounded region  $U$  and into a collection of one or more bounded regions. We note that the boundary of  $P$  has to be contained in  $U$ . Let  $R$  be the collection of ridge edges whose projection onto  $\Pi_0$  separates  $U$  from the rest of  $\Pi_0$ . For every edge  $e$  of  $R$  we pick that incident facet of  $\mathcal{E}_u$  whose projection onto  $\Pi_0$  is contained in  $U$ . We call this facet the outer facet of  $e$ . We use (the supporting planes of) the outer facets to extend the outer facets and cover the complement of  $U$  by a roof  $\mathcal{R}_1$  such that every point on  $\mathcal{R}_1$  is linked to  $R$  by a strictly monotone path.

Let  $\mathcal{R}_2$  be those portions of  $\mathcal{E}_u$  which project onto  $U$ . It is easy to see that  $\mathcal{R} := \mathcal{R}_1 \cup \mathcal{R}_2$  forms a natural roof over  $P$ . Every point of  $\mathcal{R}_2$  — including any point on  $R$  — is linked to the boundary of  $P$  by a strictly monotone path. (After all,  $\mathcal{R}_2$  does not contain a cycle of ridge edges except for  $R$ .) Since every point of  $\mathcal{R}_1$  is linked to  $R$  by a strictly monotone path, we conclude that  $\mathcal{R}$  is a natural roof. This yields a contradiction since at least some parts of  $\mathcal{R}_1$  lie above  $\mathcal{E}_u$ .  $\square$

**Corollary 23.** *The upper envelope  $\mathcal{E}_u$  of  $\mathcal{A}(P)$  is the maximum-volume natural roof over  $P$ .*

We note that Lemma 22 does not contradict the problem illustrated in Fig. 4: While indeed the upper envelope of two natural roofs need not be a natural roof,

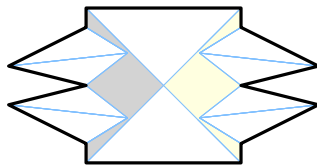


Fig. 9. The upper envelope of all natural roofs forms a natural roof.

the upper envelope of all natural roofs is a natural roof again. Figure 9 shows the upper envelope of all natural roofs (and therefore also the maximum-volume roof) for the sample polygon of Fig. 4.

We form the upper envelope  $\mathcal{R}$  over all roofs over  $P$ . Note that  $\mathcal{R}$  is a roof of maximal height and maximum volume. Now assume  $\mathcal{R}$  contains a sink, i.e., is not a natural roof. We can manually remove a sink from  $\mathcal{R}$  by applying the strategy described in the proof of Lemma 22. By repeatedly removing all sinks, we can convert  $\mathcal{R}$  into a new natural roof  $\mathcal{R}'$  without decreasing either height or volume. Since  $\mathcal{R}'$  is at every point not below  $\mathcal{R}$ , we can conclude that  $\mathcal{R}'$  is the unique upper envelope and therefore equals  $\mathcal{R}$ , which does not have a sink.

Hence, excluding roofs containing sinks from the upper-envelope construction does not affect the upper envelope, which establishes the following:

**Corollary 24.** *The maximum-volume natural roof over  $P$  is also a roof of maximum height over  $P$ .*

Note that above observation also implies that the maximum-volume roof is a natural roof.

#### 4. Plane Sweep for Min-/Max-Volume Roofs

The characterization established in the previous section suggests that roofs with minimum or maximum volume can be established by processing all mandatory and some optional admissible wavefront events, where the optional events are used for decreasing or increasing the volume of the roof. Lemma 8 tells us that every wavefront event occurs at the common intersection point of three offset supporting lines of  $P$ . Since every such intersection point corresponds to the intersection of three bisectors of edges of  $P$ , a naïve approach to computing min-/max-volume roofs would be to (1) determine all intersections among all pairs of bisectors, and (2) to process them in sorted order. This approach would result in at least  $\mathcal{O}(n^4 \log n)$  time and  $\mathcal{O}(n^4)$  space for an  $n$ -vertex polygon  $P$ .

In the sequel we derive a better algorithm by employing a plane sweep. We have already seen that the wavefront at time  $t$  corresponds to the projection of  $\mathcal{C}_t := \mathcal{R}(P) \cap \Pi_t$  onto  $\Pi_0$ . An event point in the wavefront propagation is formed by the intersection of three offset supporting lines. The respective vertex in the roof  $\mathcal{R}(P)$  is formed by the intersection of the corresponding half-planes. Intersecting one half-plane  $\Pi(e)$  with all other half-planes induced by edges of  $P$  gives rise to an

arrangement of half-lines within  $\Pi(e)$ . All half-lines in this arrangement are called *arrangement lines* of the *line arrangement* of  $\Pi(e)$ . Every arrangement line stores a reference to its current left and right roof facet. The intersection of two arrangement lines of one line arrangement corresponds to the intersection of the three half-planes (i.e., roof facets) in a common point. Hence, employing a bottom-up line sweep over all  $n$  line arrangements provides all event points. These event points correspond to all intersection points of  $\mathcal{A}^c(P)$ .

Of course, we can combine the  $n$  individual line sweeps within the  $n$  line arrangements to one plane sweep. Within every line arrangement we maintain a left-to-right order of its arrangement lines (with respect to the current height of the sweep plane) as its sweep-line status. The event points are stored in an event queue, which is a priority queue sorted by the event time.

We start the plane sweep by placing the horizontal sweep plane at  $t = 0$ . All arrangement facets that cover portions of the boundary of  $P$  are added to the roof. These arrangement facets can be found by traversing the initial sweep-line status of every half-plane. Also, the intersection points between neighboring arrangement lines in the status are computed and added as event points to the event queue.

Next, we start moving the sweep plane upwards by processing the event points stored in the event queue. At every event point we can decide locally whether we add or disregard an arrangement facet. This local decision can be drawn from the roof facets referenced by the intersecting arrangement lines. Additionally, every sweep-line status is adapted and new event points are computed and added to the event queue. During the plane sweep all edge events, split events and vertex events are handled similarly to the wavefront propagation: An edge event occurs when a roof facet ends locally and a split event occurs when a valley formed by two roof facets crashes into another roof facet. A vertex event occurs when two or three valleys meet in a common point.

A create event occurs when a valley formed by two roof facets intersects a half-plane, or two half-planes intersect a roof facet, both in a common point, and so new roof facets can be added to the roof at the event point. Recall that we have two different scenarios for create events; cf. Fig. 5: A create event occurs either on an edge or at a vertex in  $\mathcal{W}_P(t)$ . Note that for a create event to occur at the intersection of two roof facets, the intersection has to form a valley, i.e., the respective wavefront vertex must be reflex as stated in Lemma 9. Considering that the event point has to be part of the roof, and that in general position exactly three half-planes meet in a common point we can add at most two arrangement facets to the roof at the event point.

#### 4.1. Minimizing and maximizing the roof volume

We use create events for minimizing or maximizing the volume of our natural roof: At every create event we analyze whether this event adds facets with locally greater or smaller slope than the facets currently expanding there. Obviously, the roof

volume is increased (decreased, resp.) if a facet with greater (smaller, resp.) slope is added. Thus, to find the minimum-volume natural roof we only take create events that add facets which reduce the volume, that is, which locally have lower slope compared to the current facet, and ignore all other create events. We apply the opposite strategy when computing the maximum-volume natural roof. We use the following two lemmas to recognize the appropriate events during the sweep: We categorize the create events as (locally) reducing (minimizing) or increasing (maximizing) the roof volume.

**Lemma 25.** *A create event at a point  $p$  corresponds to a local reduction of the roof volume if  $p$  lies on the interior of an edge of the wavefront.*

**Proof.** Figure 5 shows that the scenario depicted in Fig. 5(i) is the only scenario that reduces the roof volume: If the create event occurs at a point  $p$  in the interior of a wavefront edge, then this edge is split and two new edges are introduced. These two new edges correspond to two new roof facets that form a valley in the roof, as the intersection of the two half-planes that support these new roof facets has a smaller slope than the constant slope of a half-plane itself. This valley replaces a portion of the half-plane and, thus, reduces the volume of the roof locally.  $\square$

The other three scenarios for a create event shown in Figs. 5(c), 5(e) and 5(g) can be used for both minimizing and maximizing. In the scenarios shown in Figs. 5(e) and 5(g), a new roof facet is added and thus one valley is replaced by another valley having a lower slope and by a ridge. Figure 5(c) shows the only scenario that increases the roof volume: the event also adds a new roof facet but in this case this change replaces one valley by two valleys both having a greater slope. In the following we establish the claim that a greedy approach combined with the (local) knowledge of a create event is sufficient to compute the global minimum (maximum).

**Theorem 26.** *A greedy algorithm can be used to compute the minimum-volume or maximum-volume natural roof of an  $n$ -vertex polygon  $P$  in  $\mathcal{O}(n^3 \log n)$  time and  $\mathcal{O}(n^2)$  space.*

**Proof.** Corollary 17 and Corollary 20 tell us that there exists a wavefront propagation which results in the minimum-volume natural roof over  $P$ .

All roofs start at the boundary of  $P$ . At every optional admissible wavefront event we check whether accepting it will result in a locally lower roof. In that case we accept it and modify the wavefront accordingly. Since the order in which the admissible wavefront events occur corresponds to a  $z$ -ordering of the roof vertices, this simple greedy approach will generate  $\mathcal{E}_\ell$ . Similar arguments in conjunction with Corollary 23 establish that a greedy approach will generate  $\mathcal{E}_u$ .

As in the case of straight skeletons we know of no way to predict whether an event will actually be admissible prior of reaching it with the sweep plane. Therefore, we have to consider all potential event points.

A classic line sweep over  $n$  lines takes linear space and  $\mathcal{O}(n^2 \log n)$  time. Every input edge  $e$  of  $P$  defines a half-plane  $\Pi(e)$ . Such a half-plane is intersected by, at most, every other half-plane of  $P$ . This results in  $\mathcal{O}(n)$  half-lines formed by the intersection of  $\Pi(e)$  with all other half-planes of  $P$ .

By running a plane sweep, we perform a line sweep for all  $n$  half-planes of  $P$ . Therefore, we need quadratic space and  $\mathcal{O}(n^3 \log n)$  time to perform the sweep.  $\square$

One can argue that no vertex events will occur when maximizing the roof volume. Hence, a lengthy analysis allows to conclude that a modification of the basic straight-skeleton algorithm by Aichholzer *et al.*<sup>1</sup> is applicable, which runs in  $\mathcal{O}(n^3)$  time and consumes  $\mathcal{O}(n)$  space. The handling of all create events can be done in  $\mathcal{O}(n^3 \log n)$  time without the need for storing many events. Hence, while maintaining the same  $\mathcal{O}(n^3 \log n)$  time complexity for computing a maximum-volume natural roof, one could get away with an output-sensitive space complexity. Since the overall savings are rather moderate we refrain from diving into lengthy details.

## 5. Simple Polygons and Definition Refinement

Our general-position assumption was that the polygon  $P$  does not contain parallel edges and that no more than three bisectors intersect in a common point. These assumptions allowed us to avoid degenerate cases in our line of reasoning. Now we are ready to waive the general-position assumption and sketch how to handle degenerate cases.

A bisector graph can be seen as a *directed bisector graph* by letting every arc inherit the orientation of its supporting bisector (ray). However, parallel input edges may lead to horizontal line segments in the roof; the corresponding bisectors are not directed. Thus, a directed bisector graph may contain undirected cycles; see Fig. 11.

In the following we describe the event handling if parallel input edges are present. Our approach follows the description of Biedl *et al.*<sup>8</sup> Suppose that two roof facets  $f_1$  and  $f_2$  intersect and that their associated half-planes originate from parallel edges,  $e_1$  and  $e_2$ , of  $P$ . If  $e_1$  and  $e_2$  move towards each other during the wavefront propagation then  $e_1$  and  $e_2$  have a bisector, and both facets end locally at their intersection  $f_1 \cap f_2$ . Now suppose that two edges  $e_1$  and  $e_2$  of  $P$  are collinear, moving into the same direction during the wavefront propagation, and that their roof facets  $f_1$  and  $f_2$  become adjacent due to an event. Then the event point is considered as the starting point of a bisector ray perpendicular to  $\ell(e_1)$ . The bisector between  $\ell(e_1)$  and  $\ell(e_2)$  is not well defined since all points in  $\mathcal{I}(e_1)$  are equidistant from both supporting lines. Thus, the vertex  $v$  in the respective roof that traces out this

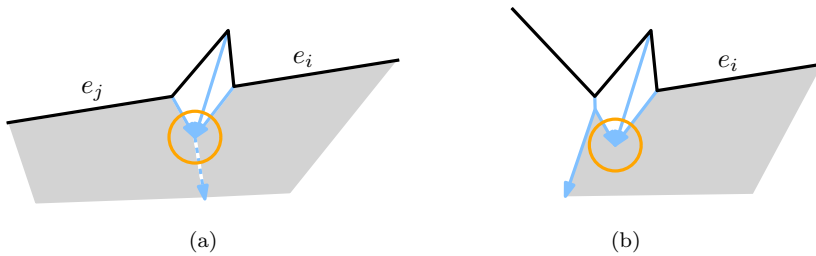


Fig. 10. In (a), we see an event where two wavefront edges collapse and two wavefront edges with common offset supporting line (but different input edges) become adjacent: A ghost vertex is created at the collapse point. The scenario in (b) looks similar but since both wavefront edges stem from the same input edge (due to a create event that had happened before) no ghost vertex is traced.

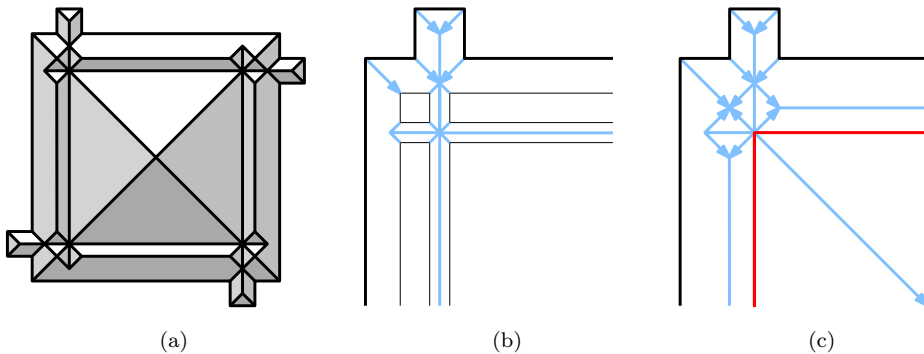


Fig. 11. In (a), we see a finished roof model of this input; in (b), we see a state of the wavefront propagation; in (c), we see the bisector graph, with the (red) inner undirected segments marking the undirected cycle in the full graph (color online).

intersection during the plane sweep is similar to a *ghost vertex*.<sup>c</sup> Thus  $v$  is defined to start at the point where  $f_1$  and  $f_2$  become adjacent during the plane sweep. The direction of  $v$  is then perpendicular to  $\ell(e_1)$  and moves on  $\Pi(e_1)$ , thereby forming an edge between  $f_1$  and  $f_2$ . Since  $e_1$  and  $e_2$  are collinear, this also means that  $v$  is perpendicular to  $\ell(e_2)$  and moves on  $\Pi(e_2)$ . (See Fig. 10 for an example of what a respective bisector graph may look like.) If the notion of ghost vertices is not used, then facets of this type would be joined together, which may result in a bisector graph with disconnected components.

The second general position assumption states that at most three planes intersect in a point  $p := \Pi(e_i) \cap \Pi(e_j) \cap \Pi(e_k)$ . All wavefront events (edge-, split-, vertex-, and create event) that only involve the intersection of three planes at the event point are called *elementary*.<sup>9</sup> All other event points, where four or more planes intersect in a common point, are classified *non-elementary*. Since non-elementary

<sup>c</sup>A ghost vertex, defined by Biedl *et al.*,<sup>8</sup> traces an edge that has the same face on both sides.

events also include the vertex event known from the straight skeleton computation<sup>3</sup> we need to revisit and generalize Definition 12.

**Definition 14 (Vertex Event\*).** A wavefront event at a point  $p$  of the wavefront is a *vertex event* if two or more wavefront vertices meet at  $p$  all of which are reflex.

Clearly this vertex event is still a mandatory wavefront event, its main difference compared with the other mandatory events is that it can produce outgoing reflex wavefront vertices.

Handling non-elementary wavefront events is discussed by Biedl *et al.*<sup>9</sup> Roughly, to handle a non-elementary event at a point  $p$  one looks at the cyclic order of the incident (non-zero length) wavefront edge pairs. The event is processed by changing the adjacency of every edge in each pair to its cyclic neighbor. This approach is applicable for straight skeleton events. Since edge and split events replace reflex vertices of the wavefront with convex vertices, no create event can occur at the same point; recall Lemma 11. To generalize the above approach to include create events, we decide that mandatory events are handled first since (i) the planarity of the wavefront depends on them and (ii) all events with the exception of create events remove either reflex wavefront vertices or wavefront edges.

In the following we analyze a non-elementary create event that takes place at a point  $p$ . When maximizing the roof volume, we insert a new zero-length edge into the wavefront for every incident offset supporting line (that is maximizing), replacing one reflex vertex of the wavefront with two reflex vertices in the process; cf. Fig. 5(c). Assuming all involved offset supporting lines have unique orientation, many such changes can be done independently, in arbitrary order: an offset supporting line that was able to contribute a new maximizing edge at point  $p$  will still have that property after we added another wavefront edge and replaced one reflex wavefront vertex by two new reflex vertices in the wavefront. If relevant offset supporting lines are collinear, we can pick any of them as the base of the new wavefront edge as the roof volume will be independent of this choice. See an example for a maximizing non-elementary create event in Fig. 12(f).

When minimizing the roof volume, every (elementary) create event results in exactly one outgoing reflex wavefront vertex as well as one or two convex wavefront vertices and inserts one or two new edges into the wavefront; cf. Figs. 5(e), 5(g) and 5(i). In a non-elementary event in the minimizing case, unlike before, not all incident offset supporting lines may be able to contribute new wavefront edges. See, for instance, the elementary create event in Fig. 12(a) and the offset supporting line that contributed a new wavefront edge in this event. In Fig. 12(b), the same offset supporting line is no longer relevant nor is it possible for it to contribute a wavefront edge when the other, new, supporting line is contributing a wavefront edge.

In order to pick the contribution(s) which minimize the total roof volume in a non-elementary create event at  $p$  where  $k$  half-planes meet, we proceed as follows: As we apply a plane sweep over the arrangement  $\mathcal{A}^C(P)$ , we can identify the  $k$

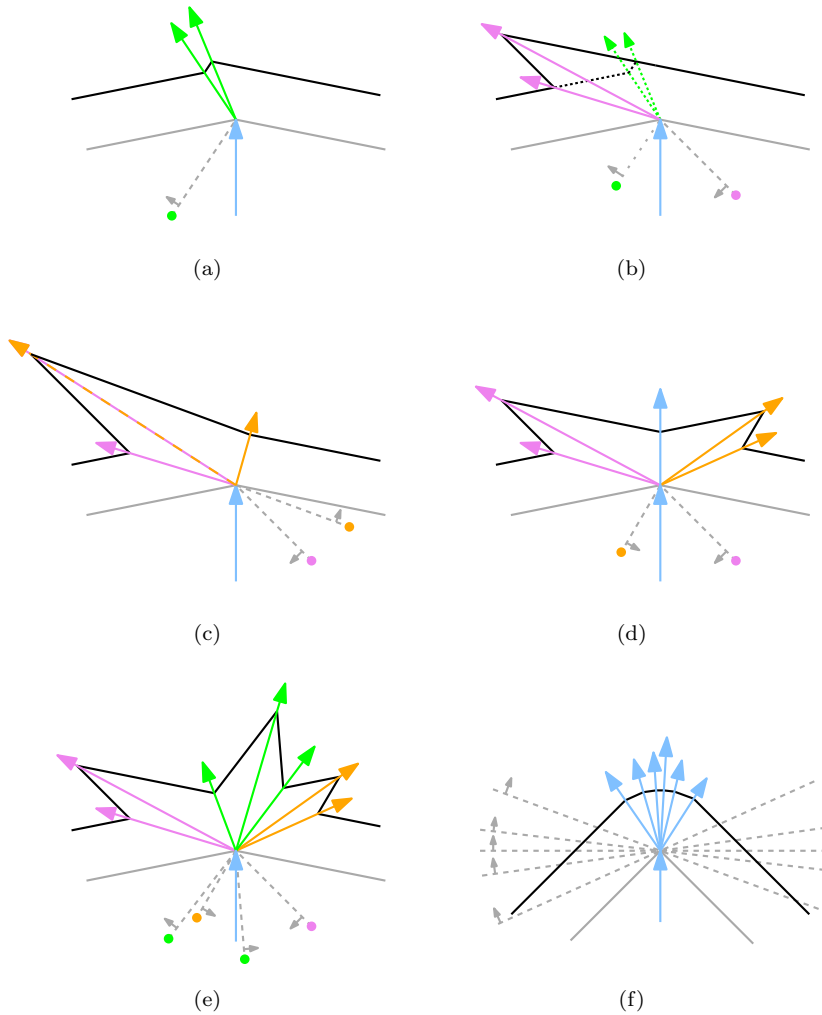


Fig. 12. In (a)–(e), we see various (non-elementary) minimizing create events, and a non-elementary maximizing create event in (f). The wavefront at the event time is drawn in gray after the event in black, incident offset supporting lines in dashed gray, bisectors are colored and the color is matched by a corresponding mark on the offset supporting lines, the orientation (relative interior) of the offset supporting lines is indicated by small gray arrows (color online).

arrangement facets that have a minimal point in  $p$ . We place a horizontal plane  $\Pi_{z(p)+\varepsilon}$  at height  $z(p) + \varepsilon$  and intersect the  $k$  arrangement facets with it, where  $\varepsilon > 0$ . This intersection is denoted  $\mathcal{C}$ . Now we find an arrangement facet that is part of a roof facet  $f$ . Since the roof is finished below  $p$ , we know the relative interior of the roof locally around  $p$ . Thus, starting at the relevant boundary edge of  $f$  we walk around  $p$  along the polygonal chain in  $\mathcal{C}$  closest or farthest away from  $p$ , depending on our applied strategy. This walk yields the appropriate facets for our minimum-volume roof.

These steps can be carried out in  $\mathcal{O}(k)$  time. Nevertheless, as we use a sweep-line status for every input edge, handling a non-elementary event with  $k$  involved half-planes takes  $\mathcal{O}(k^2)$  time: We have to reverse the order in all  $k$  sweep-line statuses and each reversal takes  $k$  time.

This cost can be amortized: Assume that a  $(k + 1)$ -st half-plane  $\Pi_{k+1}$  meets the other  $k$  half-planes in  $p$ . Then  $\Pi_{k+1}$  can not be involved in another event point with any of this  $k$  half-planes, thus excluding  $\mathcal{O}(k^3)$  other events.

### 6. Realistic Roofs

The concept of realistic roofs, by Ahn *et al.*<sup>6</sup> and Yoon *et al.*,<sup>5</sup> builds upon the roof model by Aichholzer *et al.*<sup>1</sup> However, only simple rectilinear polygons are allowed as input.

**Definition 15 (Realistic Roof<sup>5</sup>).** A realistic roof over a simple rectilinear polygon  $P$  is a roof over  $P$  satisfying the following constraints:

- (1) Every face of the roof is incident to at least one edge of  $P$ .
- (2) Every vertex<sup>2</sup> of the roof is higher than at least one of its neighboring vertices.

Every realistic roof has a linear number of facets, none of which are disconnected from their defining input edge. Furthermore, a realistic roof does not have a sink in its interior. See Fig. 13 for a comparison of a straight-skeleton induced roof and a realistic roof.

**Lemma 27.** *Realistic roofs over rectilinear polygons are a subset of natural roofs.*

**Proof.** Both concepts build on the roof model. No sinks are allowed in both natural and realistic roofs. This implies that every facet of a realistic roof fulfills the natural gradient property which makes it a natural roof as well. Furthermore, realistic roofs are, for the moment, only defined over rectilinear input polygons. Additionally, every facet is connected to at least one input line segment.

As natural roofs are defined over simple polygons and may contain disconnected facets, natural roofs clearly define a superset of realistic roofs. □

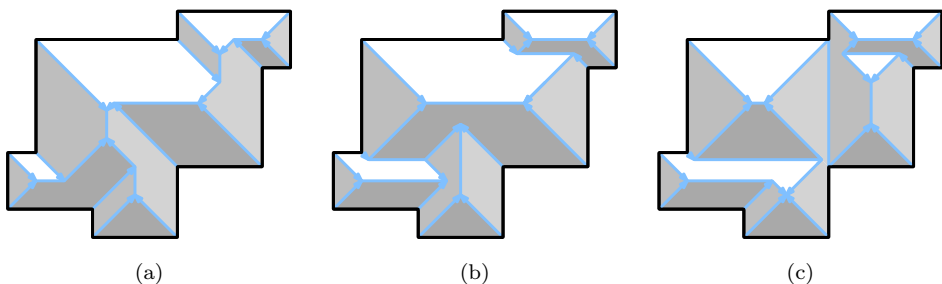


Fig. 13. In (a), we see the roof induced by the straight skeleton; in (b) a realistic roof; and in (c) the min-volume natural roof over the same polygon.

**Lemma 28.** *A minimum-volume natural roof need not be a realistic roof.*

**Proof.** See Fig. 13 for a sample polygon whose minimum-volume natural roof does not form a realistic roof.  $\square$

An algorithm to compute all realistic roofs in  $\mathcal{O}(n^5)$  time was first described by Ahn *et al.*<sup>6</sup> and later refined by Yoon *et al.*<sup>5</sup> The main idea is to search for *candidate pairs/triples*. Roughly speaking, a candidate pair (triple, resp.) consists of two (three, resp.) reflex input vertices and can be used to construct an additional valley in the roof. They differentiate between *open*, *half open* and *closed* valleys. A valley is called open if both corners are higher than at least one of their neighboring vertices; half open if one corner has this property. In case both corners have only neighboring vertices of higher altitude they call the valley closed and do not consider it, as it forms a sink. The candidate pairs/triples have to be tested for compatibility. Essentially, this test guarantees that after a candidate pair/triple is accepted it does not result in disconnected facets in the roof. Furthermore, all pairs/triples are tested against each other to ensure that they do not intersect.

After introducing certain constraints one could use our strategy for computing natural roofs to compute a realistic roof in general. Unfortunately, our plane-sweep approach does not result in the minimum-volume realistic roof. Assume that we can utilize pairs of create events to determine (half) open valleys: Then the valley (red) in Fig. 14(b) could be computed. However, the realistic roof in Fig. 14(c) has less volume, but at the time this valley would be found during a propagation process it could not be accepted into the roof anymore: Adding the second valley to the roof would result in disconnected facets and therefore violate the definition of realistic roofs.

## 7. Combinatorial Complexity

The minimum/maximum volume roof is unique for any given input polygon  $P$ . However, this observation does not tell us anything on either the number of facets

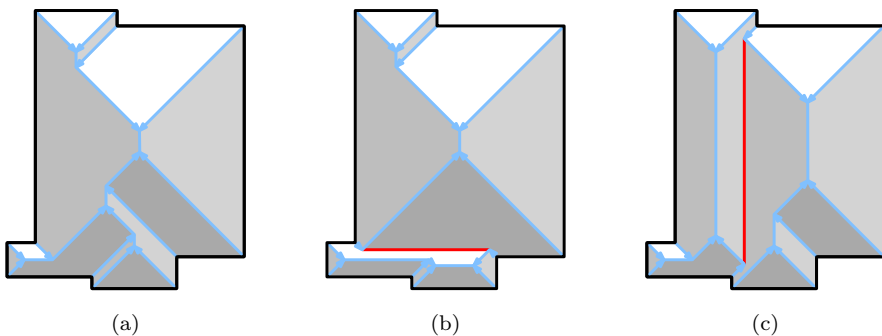


Fig. 14. In (a), we see the roof induced by a straight skeleton; in (b) and (c) we see two realistic roofs, where (c) seems to have less volume than (b). The red line marks the open valley (color online).

of such a roof or the number of different natural roofs over  $P$ . Hence, prompted by a reviewer, we conclude our paper with a short analysis of the combinatorial complexity of natural roofs.

The straight-skeleton of a simple polygon  $P$  induces a natural roof with a linear number of roof facets. If  $P$  is convex, then its straight skeleton induces the only roof over  $P$ : The offset-supporting line of any input edge  $e$  of a convex polygon  $P$  cannot interact with the wavefront except for the portion that originates at  $e$ . Hence, every convex polygon admits exactly one natural roof which has linearly many facets. Thus, this establishes tight bounds for both the number of facets and the number of natural roofs in the convex case.

Let us now focus on the polygon sketched in Fig. 15. In its lower portion it contains a linear number of spikes which emanate reflex wavefront vertices that travel upwards along vertical rays. Let  $S_l$  be the set of these spikes. The polygon also contains a set  $S_r$  of a linear number of spikes on its right-hand side which emanate reflex wavefront vertices that travel leftwards along horizontal rays. Of course, within  $\Pi_0$  all horizontal rays intersect all vertical rays, and these rays have valleys and ridges associated with them in a natural roof over  $P$ . It is crucial for our set-up that the spikes of  $S_l$  and  $S_r$  are arranged in such a way that all valleys which originate at  $S_l$  lie above all valleys of  $S_r$  but below all ridges of  $S_r$ , while all ridges of  $S_l$  lie above all ridges of  $S_r$ . Hence, in a classic straight-skeleton propagation all induced valleys/ridges of  $S_l$  end before the bottom-most ridge of  $S_r$ . This property can be guaranteed by fine-tuning the interior angles at the spikes and their relative positions.

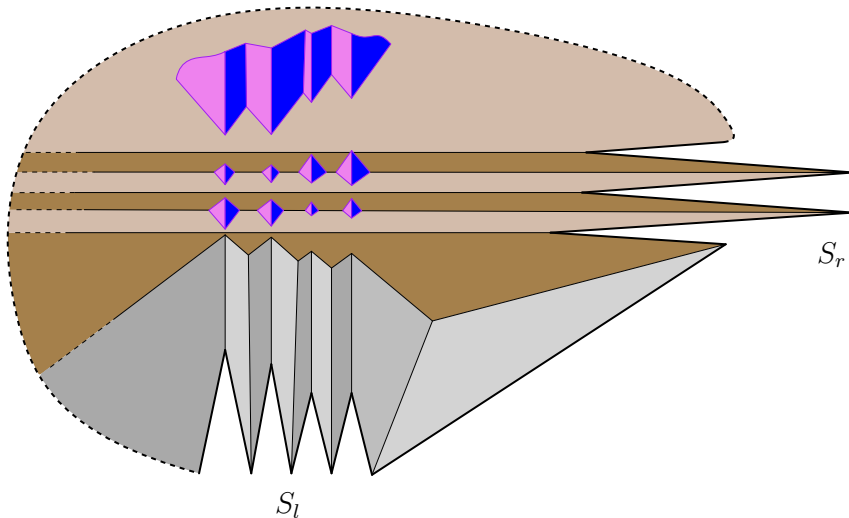
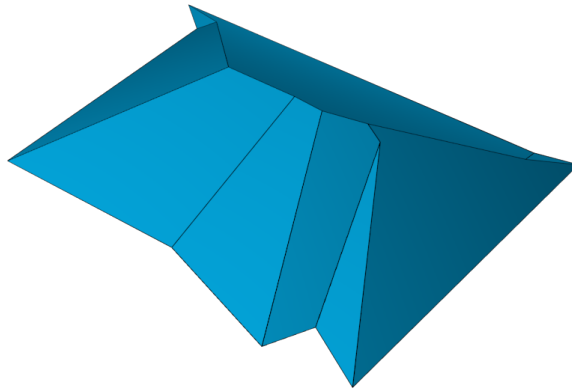
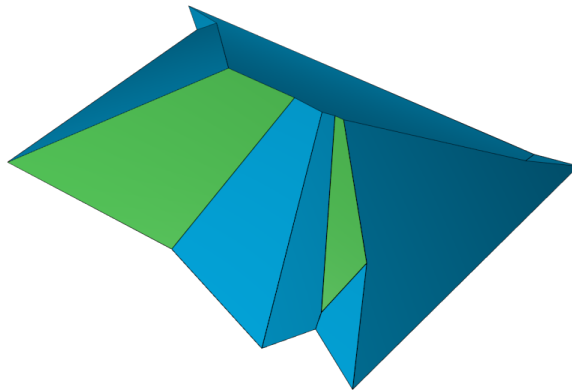


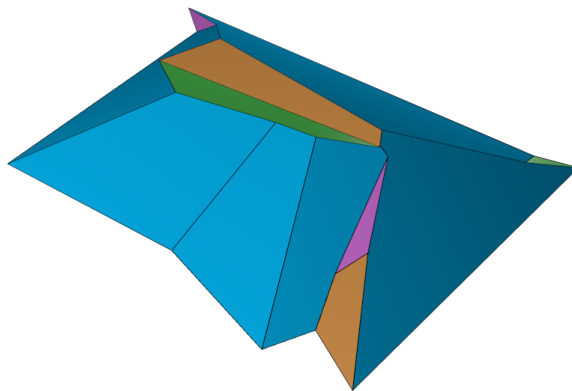
Fig. 15. Portion of a natural roof with a quadratic number of roof facets (color online).



(a)



(b)



(c)

Fig. 16. In (a), we see a straight skeleton roof, in (b) the maximum-volume natural roof, and in (c) the minimum-volume natural roof over the same input polygon.

Due to this set-up, a create event is possible between every valley of  $S_l$  and every ridge of  $S_r$ . Such a create event results in cutting a v-shaped notch out of the two facets that are incident at the ridge. (In Fig. 15, the notches are shown by purple/blue shading.) Furthermore, all these create events are independent from each other. Hence we get a quadratic number of possible facets due to a quadratic number of create events. By construction, every roof obtained by applying one or more such create events is a natural roof.

We conclude that the minimum-volume natural roof of an  $n$ -vertex polygon may have  $\Theta(n^2)$  many facets. Furthermore, there exists polygons that admit  $\Omega(2^{\Theta(n^2)})$  different natural roofs. For comparison purposes, we recall that  $1.3211^m \cdot \binom{m}{\lfloor m/2 \rfloor}$ , where  $m := (n-2)/2$ , constitutes an upper bound<sup>5</sup> on the number of realistic roofs over a rectilinear polygon with  $n$  vertices.

## 8. Implementation

We implemented our algorithm in C++11 using CGAL<sup>10</sup> version 4.9, based on the `Exact_predicates_exact_constructions` kernel with the `sqrt` extension. The source code and example test data sets are freely available on github.com: <https://github.com/guenthereder/roofer>. A rendered output computed by our implementation is shown in Fig. 16 for the bisector graphs of Fig. 2.

## Acknowledgments

This work was supported by Austrian Science Fund (FWF): Grants P25816-N15 and ORD 53-VO. Thanks go to a reviewer for the suggestion to discuss bounds on the number of different natural roofs.

## References

1. O. Aichholzer, F. Aurenhammer, D. Alberts and B. Gärtner, A novel type of skeleton for polygons, *J. Universal Comp. Sci.* **1** (1995) 752.
2. G. A. von Peschka, *Kotirte Projektionsmethode (Kotirte Ebenen) und deren Anwendung* (Buschak & Irrgang, Brünn, 1882).
3. D. Eppstein and J. Erickson, Raising roofs, crashing cycles, and playing pool: Applications of a data structure for finding pairwise interactions, *Discr. Comput. Geom.* **22** (1999) 569.
4. S.-W. Cheng, L. Mencil and A. Vigneron, A faster algorithm for computing straight skeletons, *ACM Trans. Algorithms* **12** (2016) 44:1.
5. S. D. Yoon, H.-K. Ahn and J. Sherrette, Realistic roofs without local minimum edges over a rectilinear polygon, *Theor. Comp. Sci.* **675** (2017) 15.
6. H.-K. Ahn, S. W. Bae, C. Knauer, M. Lee, C.-S. Shin and A. Vigneron, Realistic roofs over a rectilinear polygon, *Comput. Geom. Theor. Appl.* **46** (2013) 1042.
7. O. Aichholzer and F. Aurenhammer, Straight skeletons for general polygonal figures in the plane, *Proc. 2nd Int. Comput. and Combinat. Conf.*, eds. J.-Y. Cai and C. Wong, Lecture Notes in Computer Science, Vol. 1090 (Springer, Berlin, Heidelberg, Hong Kong, 1996), pp. 117–126.

8. T. Biedl, M. Held, S. Huber, D. Kaaser and P. Palfrader, Weighted straight skeletons in the plane, *Comput. Geom. Theor. Appl.* **48** (2015) 120.
9. T. Biedl, S. Huber and P. Palfrader, Planar matchings for weighted straight skeletons, *Int. J. Comput. Geom. Appl.* **26** (2016) 221.
10. The CGAL Project, *CGAL User and Reference Manual* (CGAL Editorial Board, 2016), 4.9 edition.